Nanostructuring of NiMnSb(110): Influence on surface magnetic properties

Ch. Eickhoff,[*] H. Kolev,[†] M. Donath, G. Rangelov,[‡] and L. F. Chi

Physikalisches Institut, Westfälische Wilhelms-Universität Münster, Wilhelm-Klemm-Strasse 10, 48149 Münster, Germany

The magnetic properties, crystal structure, and topography at the (110) surface of the ferromagnetic half-Heusler alloy NiMnSb have been investigated by means of magneto-optical Kerr effect, spin-resolved appearance potential spectroscopy, low-energy electron diffraction, and atomic force microscopy. A standard sputter-anneal cleaning procedure leads to a nanostructuring of the surface with consequences for the magnetic properties. This finding sheds light on the reduced spin polarization measured by surface-sensitive techniques on NiMnSb surfaces.

PACS number(s): 75.60.−d, 68.35.Bs, 75.75.+a, 78.20.Ls

I. INTRODUCTION

Half-metallic ferromagnets are a class of materials with very interesting properties. At the Fermi level E_F, electronic states of only one spin orientation exist. Therefore, 100% spin polarization is expected at the Fermi level. This behavior is promising for spin injection applications in magneto-electronic and spintronic devices. In this respect, some Heusler alloys are possible candidates. They are ternary cubic phases X_2YZ (Heusler alloys) or XYZ (half-Heusler alloys), where $X=\mathrm{Ni},\mathrm{Co},\mathrm{Pt},\ldots$, $Y=\mathrm{Mn},\mathrm{Sr},\ldots$, and $Z=\mathrm{Sb},\mathrm{As},\ldots$.[1] For NiMnSb, as an example, a 0.5 eV band gap was predicted for the minority electrons at E_F at $T=0$ K.[2] With a Curie temperature of about 730 K, the magnetization at room temperature amounts to $\approx 92\%$ of the saturation value.[3] The impact of the temperature-dependent magnetization on the band gap and the spin polarization at E_F is not clear at present.[4] Nevertheless, together with the small lattice mismatch to current III-V semiconductors, NiMnSb is a very promising candidate for device applications.

A variety of experimental results for NiMnSb is available in the literature. While bulk measurements support the half-metallic behavior (see, e.g., Refs. 5 and 6), surface- and interface-sensitive techniques failed so far to detect the energy gap for minority electrons or the 100% spin polarization at the Fermi level E_F. By Andreev reflection[7] or spin-resolved photoemission,[8] a spin polarization of only $\approx 50\%$ was observed. A study by angle and spin-resolved inverse photoemission reported close to 100% spin polarization at E_F under certain conditions.[18] Kolev *et al.*[9] reported that the spin asymmetry measured by appearance potential spectroscopy, a technique sensitive to the density of unoccupied states above E_F, is less than half the value predicted by theory.

In the literature, a number of reasons are discussed which could be responsible for a reduced spin polarization and/or asymmetry from the surface: a crossover from a half-metallic ferromagnet to a normal metallic ferromagnet near 80 K,[10] a band gap smaller than 0.5 eV,[11] the existence of surface states,[13–15] or the possibility that the NiMnSb surfaces do not exhibit a half-metallic behavior as a result of the symmetry break at the surface.[16,17] Besides these more fundamental issues, it is not a trivial experimental task at all to prepare a clean and stoichiometric surface of NiMnSb. Surface segregation has to be carefully considered.[12] In addition, the reduced spin polarization observed in surface-sensitive experiments may be a result of a reduced magnetization at remanence compared with the saturation value. Electron spectroscopies with spin resolution rely on a defined magnetic state of the sample in remanence because, in general, no external fields can be applied to saturate the sample. A reduced magnetization in remanence can be caused, e.g., by a complex magnetic (surface) domain structure.[8,9] For this, the intrinsic and induced magnetic anisotropies have to be taken into account.[19,20]

According to the literature, the $\langle 111 \rangle$ directions are the easy magnetization axes in NiMnSb.[21] Therefore, the former studies on a NiMnSb(001) surface[9] and on polycrystalline samples[8] were hindered by the fact that the surfaces under investigation did not contain an easy magnetization axis in the surface plane. This motivated us to investigate the (110) surface of a NiMnSb single crystal, which contains $\langle 111 \rangle$ directions in the surface plane. As a consequence, it should be easier to achieve magnetic saturation in remanence, thereby avoiding complex magnetic closure domains at the surface. Magnetic saturation in remanence or at least a defined domain structure is necessary for a quantitative determination of the electron spin polarization or asymmetry. However, the (110) surface is the most open surface of the low-index surfaces (111), (001), and (110), which may complicate the preparation of a stoichiometric surface with a good crystallographic order. Therefore, we explored the NiMnSb(110) crystal with a combination of techniques able to characterize the surface structure and composition as well as the magnetic properties.

II. EXPERIMENTAL DETAILS

For our studies, we used an ultrahigh vacuum (UHV) system with a base pressure of about 5×10^{-11} mbar. Low-energy electron diffraction (LEED) and Auger-electron spectroscopy (AES) with a four-grid retarding-field analyzer were used as standard techniques to control the surface quality with respect to crystallographic structure and composition. Information about the topographic surface structure was obtained by an *extra situm* atomic force microscope (AFM). We applied the longitudinal magneto-optical Kerr effect (MOKE), *extra situm* as well as *in situ*, in order to study the

magnetic properties. Furthermore, the domain formation was monitored using an *extra situm* Kerr microscope. External magnetic fields with maximum values of 825 G (MOKE) and 925 G (Kerr microscope) were applied. The spin-dependent density of unoccupied states was investigated via spin-resolved appearance potential spectroscopy (APS).[9,22]

The NiMnSb(110) sample was cut, polished, and oriented by MaTeck GmbH. The sample temperature was measured with a nonmagnetic thermocouple type-*D* $W_{0.97}Re_{0.03}/W_{0.75}Re_{0.25}$, directly connected to the sample surface. Since it is not a trivial task to get a well ordered and stoichiometric NiMnSb surface, we paid special attention to the sample preparation. Several preparation procedures are reported in the literature, which were used to get clean and stoichiometric single crystalline surfaces.[11,23–25] All are based on a standard sputter-anneal procedure, consisting of sputtering with Ar^+ or Ne^+ ions at various energies with subsequent annealing at a variety of temperatures. Due to preferential sputtering of Mn and Sb, the surface becomes enriched with Ni during sputtering. Subsequent annealing for several minutes is necessary to recover a stoichiometric surface via the segregation of Mn and Sb. In our study on the (110) surface, "gentle" sputtering with 600 eV Ar^+ ions plus annealing at 600 K for several minutes turned out to be unsuccessful for a clean surface with bulk composition. Therefore, we increased the sputter energy to 1000 eV. The annealing process was modified to 700 K for 30 min. After many cycles of this procedure, we were able to observe sharp LEED patterns with low background, evidence of a well-ordered surface. In addition, a recovery of a clean surface with almost bulk composition (1:1:1 for Ni:Mn:Sb) was confirmed by AES.

III. RESULTS AND DISCUSSION

Before the mechanically polished NiMnSb(110) surface was installed into the UHV chamber, we characterized the magnetic properties *extra situm*. Using MOKE with an applied field along a $\langle 111 \rangle$ crystallographic direction, we obtained the hysteresis loop shown in Fig. 1(a). The expectation of a square hysteresis loop, based on the above argument about easy magnetization axes, was not fulfilled. The magnetic field was not sufficient to reach magnetic saturation. Also, low remanence was observed. This behavior was studied in more detail by Kerr microscopy. The remanent magnetic state showed a complex domain structure at the surface. Even though the applied field was higher in the microscope, saturation magnetization could not be achieved.

We monitored the evolution of the magnetic behavior with *in situ* MOKE with increasing number of preparation cycles in UHV. Surprisingly, the MOKE signal became gradually smaller. As a criterion for the change of the MOKE signal, we used the signal-to-noise (S/N) ratio. It was obtained from a division of the Kerr rotation by the noise (standard deviation) of the curves, taking into account the different measuring times. A ratio of $S/N=24$ was obtained for the nonbombarded and nonannealed sample, but only $S/N=2$ for the clean and well-ordered sample after many preparation cycles. Aside from this negative development, the shape of
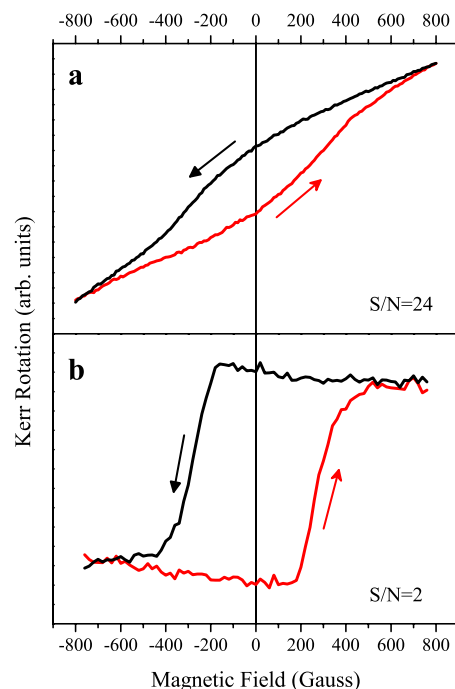

FIG. 1. (Color online) MOKE hysteresis loops of NiMnSb(110). The magnetic field was applied along a $\langle 111 \rangle$ crystallographic direction. (a) *Extra situm* measurement after crystal polishing. (b) *In situ* measurement after many cycles of Ar^+ ions bombardment and annealing.

the hysteresis loop changed in a promising way; it became almost rectangular. The coercive field decreased to about 290 G, and the remanent magnetization was observed almost equal to the saturation value [see Fig. 1(b)]. The slightly larger remanence compared to the saturation magnetization is attributed to a small misalignment of the experimental MOKE setup.

In summary, the magnetic properties of the NiMnSb(110) surface responded strongly to the increasing number of preparation cycles. Though the overall MOKE signal decreased, the shape of the hysteresis changed toward a rectangular loop. We assume that the sputter-anneal cycles released mechanical stress caused by the polishing procedure of the crystal. As a consequence, the strain-induced magnetic anisotropy was lowered and the crystalline anisotropy took over in a way that the $\langle 111 \rangle$ crystallographic directions become the easy magnetization axes. However, the strongly reduced MOKE signal came as a surprise and will be discussed later.

With this promising change of the magnetic properties in mind, we investigated the spin dependence of the density of unoccupied states by spin-resolved APS. Equivalent studies on a NiMnSb(001) surface with its complex magnetic domain structure had resulted in a spin asymmetry of $A=-0.115\pm0.012$ in the Mn $2p_{3/2}$ excitation line.[9,24] This result, which was even an extrapolated value for a sample with hypothetically saturated magnetization, was still about a factor of 2 smaller than the theoretical value of $A=-0.25$ predicted for the half-metallic ferromagnet NiMnSb.[9] From NiMnSb(110), with its better defined magnetic structure, we expected a spin asymmetry closer to the theoretical predic-
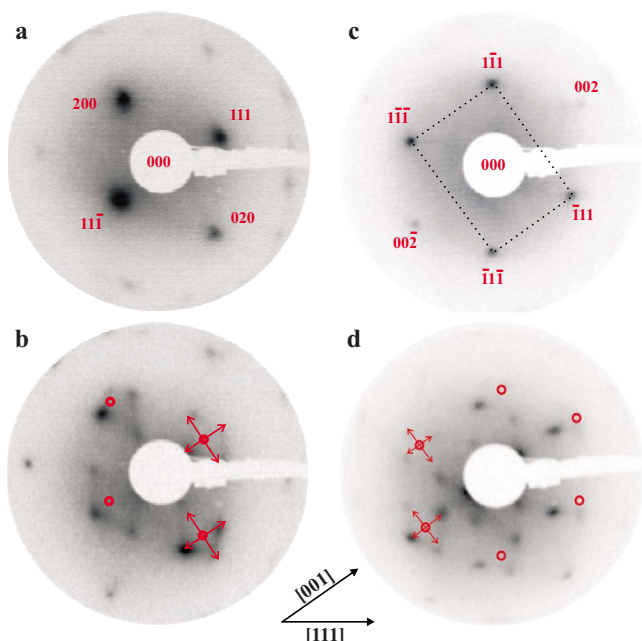
FIG. 2. (Color online) LEED patterns of NiMnSb(110), recorded at 58 eV (a) and a few eV above 58 eV (b), at 85 eV (c) and a few eV above 85 eV (d). Open circles in (b) and (d) represent the LEED spots recorded at 58 and 85 eV, respectively, taken from (a) and (c). The split spots move in $\langle 100 \rangle$ and $\langle 110 \rangle$ crystal directions. They are interpreted as LEED patterns from facets with {111} and {100} surface orientations (see text). The numbers indicate the coordinates of the reciprocal lattice points associated with the LEED spots.

tion. However, our experiments gave a value of only $A = -0.058 \pm 0.014$, even further away from the theoretical prediction. Although the sample surface exhibits the correct bulk composition, probed by AES, and an almost rectangular hysteresis curve, probed by MOKE, the spin asymmetry of the APS signal is strongly reduced.

To understand this unexpected result, we have to focus on the surface crystallographic order and its topography in more detail. With the cleaning procedure described above, we arrived at sharp LEED patterns for electron energies of 58 and 85 eV, as shown in Figs. 2(a) and 2(c). The horizontal axis is parallel to the [111]-crystal direction, which includes an angle of 35.3° with the [001] direction. The plotted rectangle in Fig. 2(c) shows an aspect ratio of 1:1.4. This observation agrees well with the expected pattern for a (110) surface, a rectangle with an aspect ratio of $1 : \sqrt{2}$.

However, we observed these kinds of "simple" LEED patterns only for certain electron energies. For other electron energies, the LEED patterns showed additional spots moving in different directions as the electron energy was varied. With increasing energy, we observed the expected converging of the main LEED spots toward the center, characteristic of a surface oriented perpendicular to the impinging electron beam. Yet, in addition, we saw the spots from the (110) surface splitting up into four spots, diverging along the $\langle 100 \rangle$ and $\langle 110 \rangle$ directions [Figs. 2(b) and 2(d)]. For reasons of comparison, the open circles in Figs. 2(b) and 2(d) indicate the positions of the LEED spots from Figs. 2(a) and 2(c).

With increasing electron energy starting from 58 eV, we observe the spots splitting up into multiple spots and then converging to a simple LEED pattern again at 85 eV. Instead of a smooth surface, we found evidence of ordered tilted planes (facets) at a length scale of at least 10 nm. The formation of facets explains the sharp LEED spots with low background at energies of 58 and 85 eV and the splitting of the spots at other energies.

If a surface plane is inclined by an angle $\neq 90°$ with respect to the incident electron beam, the respective specular beam appears away from the center of the LEED screen. In the case of facets, each facet orientation will produce a specular beam on the screen to which or from where the spots of the respective diffracted beams move. To determine the facet orientations, we followed the spot migration as a function of the electron energy. According to a recipe in the literature, the orientation of the facets can be deduced as the difference of the indices between the two points of the reciprocal lattice, which are crossed by the migrating spots, or, in other words, where the facet spots on their way coincide with the spots of the plane surface.[26] To do so, one has to assign the indices of the corresponding reciprocal lattice points to the LEED spots, which has been done in Fig. 2. As an example of spot migration, the spot denoted as 020 at 58 eV electron energy migrates with increasing energy along [00$\bar{1}$] to reach the $\bar{1}1\bar{1}$ spot at 85 eV. The difference of these two spots $(020 - \bar{1}1\bar{1} = 111)$ gives the orientation of the facet plane as (111). Another spot migrates from 111 to 1$\bar{1}$1 along the [1$\bar{1}$0] direction, which defines a second facet orientation $(111 - 1\bar{1}1 = 020)$ to (020). Following the spot migration in the various directions, this analysis leads to facet orientations of type {111} and {100}, which enclose angles α_1 and α_2 of 35.3° and 45° with the (110) surface plane, respectively.

The angles $\alpha_{1,2}$ can be deduced directly from the electron energies, at which the LEED spots of the (110) surface and the facet surfaces coincide. For details about the determination of facet orientations and the calculation of their angles with respect the flat surface, the reader is referred to the literature.[26–28] Accordingly, $\tan \alpha_{1,2}$ is given by the absolute value of the reciprocal lattice vector (between the two coincidence cases) divided by the difference between the diameters of the two Ewald spheres for the different energies. The radii of the corresponding Ewald spheres are calculated from the kinetic energies of the incoming electron beam. With the two coincidence energies, 58 ± 1 eV and 85 ± 1 eV, we arrive at angles $\alpha_1 = 33 \pm 2°$ and $\alpha_2 = 43 \pm 2°$, in good agreement with the facet orientations derived above. We conclude that the observed LEED patterns of the NiMnSb crystal after preparation clearly show a faceted (110) surface. The observed {111} and {100} facets [with two orientations relative to the (110) surface in both cases] have crystal planes, which are more closed than the open (110) surface. The tendency of the crystal to lower its surface free energy is assumed to drive the formation of lower-energy planes with {111} and {100} crystal planes. This energetically favored state is obviously achieved by repeated sputter-anneal cycles.

We report on an additional observation. With increasing number of sputter-anneal cycles, the surface color of the
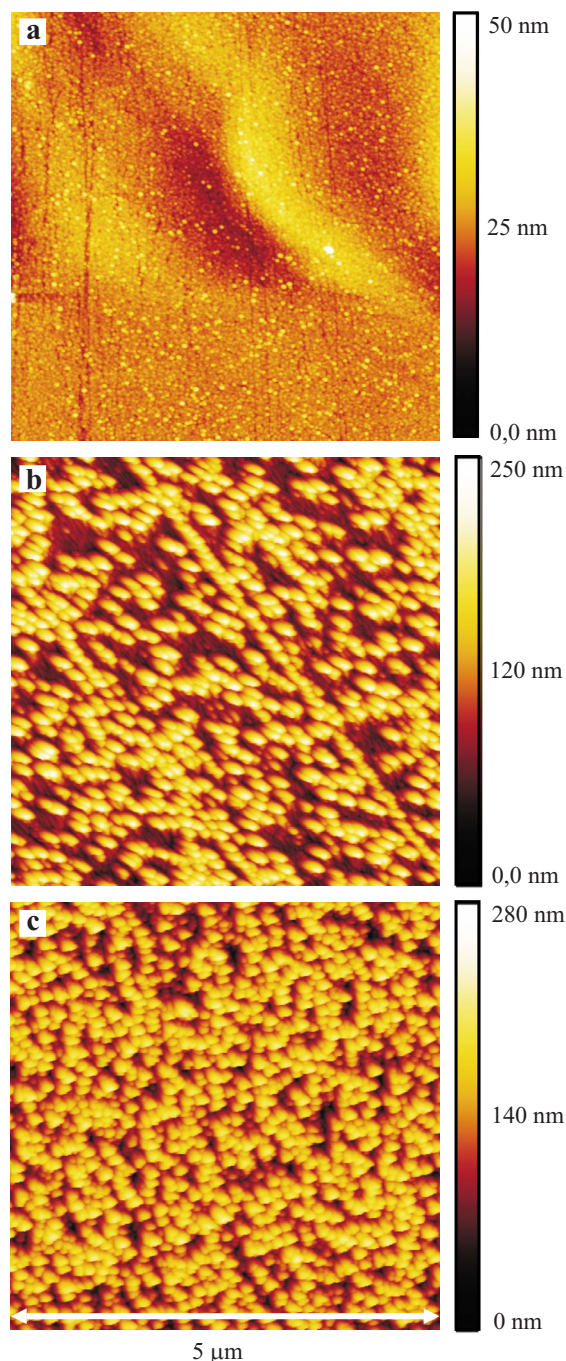
FIG. 3. (Color online) AFM pictures of three different regions of the NiMnSb(110) sample. (a) Nonsputtered region. (b) Slightly sputtered region [about half as much as in (c)]. (c) Heavily sputtered region. The lateral size of the pictures is equivalent to 5 μm. The bars on the right indicate the height of the structures.

NiMnSb sample changed from a metallic glance to a "milky" color. This led us to the hypothesis that the surface became rough and built of structures whose lateral size is in the range of optical wavelengths. To test this hypothesis, we performed AFM measurements on three different regions of the NiMnSb(110) surface. Figure 3(a) shows an AFM picture of a sample region that was not hit by the ion beam. A smooth surface can be recognized. In the second, slightly sputtered

region [Fig. 3(b)], nanodots are apparent. The third region [Fig. 3(c)] was exposed to all preparation cycles. In this region, we observed the strongest milky discoloration of the NiMnSb(110) sample. Compared with Fig. 3(b), the density of the formed nanostructures is increased. The lateral size of the structures is several hundreds of nanometers and the height is in the order of 100 nm.

The observed nanostructuring reminds us of experiments on semiconductor surfaces where nanostructures were produced by erosion sputtering.[29] An ion dose of about 4×10^{18} ions/cm^2 was used to create nanodots on a GaSb(001) surface. The ion dose that we used to obtain comparable structures on NiMnSb(110) [see Fig. 3(c)] was only about 8×10^{15} ions/cm^2. The nanostructuring leads to the discoloration of the surface, an observation also reported by Allmers *et al.* However, in our case, the nanostructures are crystallographically ordered with defined facet orientations, while the nanodots on GaSb(001) show an amorphous surface.

To summarize the consequences of our preparation cycles, we succeeded to get (i) a clean sample surface with almost bulk composition, (ii) a crystallographically well-ordered but nanostructured (110) surface with pronounced {100} and {111} facets, (iii) an easy-axis magnetic hysteresis behavior, yet with low MOKE signal, and (iv) a disappointingly low spin asymmetry of the Mn $2p_{3/2}$ signal in APS.

An additional *extra situm* investigation with the Kerr microscope after all preparation cycles was no longer possible because of the surface roughness causing a great amount of scattered light. The induced surface roughness also provides an explanation for the reduced MOKE signal described above. We understand the results as follows: For MOKE, a reflecting surface is necessary. Therefore, the detected MOKE signal does not contain information about the formed nanostructures, but only on the sample parts without nanostructures. As a consequence, we cannot study the magnetic properties of the nanostructures by MOKE because it is based on direct reflection of the incident light. APS, however, with its small probing depth of a few atomic layers, probes primarily the nanostructures with their unknown magnetic properties. We can only speculate about the magnetization of the nanostructures, which might well be influenced by shape anisotropy. With this in mind, the small spin asymmetry is no longer surprising. It may be elucidating to study the nanostructures by a local magnetic probe, which we, unfortunately, do not have in our laboratory. The goal, however, must be to find a way to prepare flat, well-ordered, and stoichiometric NiMnSb surfaces, which, as our experiment shows, are not possible to achieve by standard sputter-anneal cycles.

IV. CONCLUSION

We have investigated the surface of a NiMnSb(110) single crystal by means of MOKE, Kerr microscopy, spin-resolved APS, LEED, and AFM. With increasing number of preparation cycles, the shape of the hysteresis loop became more and more rectangular but, at the same time, the MOKE signal decreased. The LEED investigation showed the forma-

tion of {111} and {100} facets on the surface. An AFM study confirmed the appearance of nanostructures. The formed nanodots are the reason for the milky color of the sample and are made responsible for the decreasing MOKE signal. They also give an explanation for the small spin asymmetry obtained by spin-resolved APS.

By using a standard sputter-anneal procedure for preparing a NiMnSb(110) surface, we achieved a clean surface with bulklike composition, but with, for our purpose, undesirable nanostructures. Further studies on a NiMnSb(001) surface showed us that the formation of nanostructures caused by sputter-anneal cycles appears there as well, yet not as pronounced as on the (110) surface. We conclude that sputter-anneal cycles for the preparation of NiMnSb surfaces influence both the surface topography and the magnetic structure in an undesired way. This finding has to be taken into account when discussing reduced spin-polarization values obtained from NiMnSb surfaces.

*Present address: Max-Born-Institut, Max-Born-Str. 2a, 12489 Berlin, Germany; eickhoff@mbi-berlin.de

†Present address: Institute of Catalysis, Bulgarian Academy of Sciences, Acad. G. Bonchev St., Bldg. 11, Sofia 1113, Bulgaria.

‡Present address: Department für Physik, Ludwig Maximilians-Universität, Schellingstr. 4, 80799 München, Germany.

[1] P. J. Webster and K. R. A. Ziebeck, *Heusler Alloys*, Landolt-Börnstein, Numerical Data and Functional Relationships in Science and Technology, New Series, Group III, Vol. 19C (Springer, Berlin, 1988), p. 75.

[2] R. A. de Groot, F. M. Mueller, P. G. van Engen, and K. H. J. Buschow, Phys. Rev. Lett. **50**, 2024 (1983).

[3] L. Ritchie, G. Xiao, Y. Ji, T. Y. Chen, C. L. Chien, M. Zhang, J. Chen, Z. Liu, G. Wu, and X. X. Zhang, Phys. Rev. B **68**, 104430 (2003).

[4] C. N. Borca, T. Komesu, H.-K. Jeong, P. A. Dowben, D. Ristoiu, Ch. Hordequin, J. P. Nozières, J. Pierre, S. Stadler, and Y. U. Idzerda, Phys. Rev. B **64**, 052409 (2001).

[5] P. A. M. van der Heide, W. Baelde, R. A. de Groot, R. A. de Vroomen, P. G. van Engen, and K. H. J. Buschow, J. Phys. F: Met. Phys. **15**, L75 (1985).

[6] K. E. H. M. Hanssen, P. E. Mijnarends, L. P. L. M. Rabou, and K. H. J. Buschow, Phys. Rev. B **42**, 1533 (1990).

[7] R. J. Soulen, J. M. Byers, M. S. Osofski, B. Nadgorny, T. Ambrose, S. F. Cheng, P. R. Broussard, C. T. Tanaka, J. Nowak, J. S. Moodera, A. Barry, and J. M. D. Coey, Science **282**, 85 (1998).

[8] W. Zhu, B. Sinkovic, E. Vescovo, C. Tanaka, and J. S. Moodera, Phys. Rev. B **64**, 060403(R) (2001).

[9] H. Kolev, G. Rangelov, J. Braun, and M. Donath, Phys. Rev. B **72**, 104415 (2005).

[10] C. Hordequin, D. Ristoiu, L. Ranno, and J. Pierre, Eur. Phys. J. B **16**, 287 (2000).

[11] G. L. Bona, F. Meier, M. Taborelli, E. Bucher, and P. H. Schmidt, Solid State Commun. **56**, 391 (1985).

[12] D. Ristoiu, J. P. Nozieres, C. N. Borca, B. Borca, and P. A. Dowben, Appl. Phys. Lett. **76**, 2349 (2000).

[13] S. J. Jenkins and D. A. King, Surf. Sci. **494**, L793 (2001).

[14] S. J. Jenkins and D. A. King, Surf. Sci. **501**, L185 (2001).

[15] I. Galanakis, J. Magn. Magn. Mater. **288**, 411 (2004).

[16] G. A. de Wijs and R. A. de Groot, Phys. Rev. B **64**, 020402(R) (2001).

[17] S. Picozzi, A. Continenza, and A. J. Freeman, J. Appl. Phys. **94**, 4723 (2003).

[18] D. Ristoiu, J. P. Nozieres, C. N. Borca, T. Komesu, H.-K. Jeong, and P. A. Dowben, Europhys. Lett. **49**, 624 (2000).

[19] M. Donath, Appl. Phys. A: Solids Surf. **A49**, 351 (1989).

[20] K. Starke, K. Ertl, and V. Dose, Phys. Rev. B **46**, 9709 (1992).

[21] R. M. Bozorth, *Ferromagnetism* (IEEE, New York, 1993), p. 574.

[22] G. Rangelov, K. Ertl, F. Passek, M. Vonbank, S. Bassen, J. Reinmuth, M. Donath, and V. Dose, J. Vac. Sci. Technol. A **16**, 2738 (1998).

[23] W. Grentz, Ph.D. thesis, Freie Universität Berlin, 1991.

[24] M. Donath, G. Rangelov, J. Braun, and W. Grentz, in *Local-Moment Ferromagnets*, Lecture Notes in Physics Vol. 678, edited by M. Donath and W. Nolting (Springer, Berlin, 2005), p. 261.

[25] S. Plogmann, Ph.D. thesis, Universität Osnabrück, 1999.

[26] M. Henzler and W. Göpel, *Oberflächenphysik des Festkörpers* (Teubner, Wiesbaden, 1991).

[27] H. Lüth, *Surfaces and Interfaces of Solids* (Springer, Berlin, 1993).

[28] E. Wisotzki, Ph.D. thesis, Technische Universität Darmstadt, 2003.

[29] T. Allmers, M. Donath, and G. Rangelov, J. Vac. Sci. Technol. B **24**, 582 (2006).